

## FAST TRACK PAPER

# Seismic boundaries in the mantle beneath Iceland: a new constraint on temperature

L. P. Vinnik,<sup>1</sup> G. R. Foulger<sup>2</sup> and Z. Du<sup>3</sup>

<sup>1</sup>*Institute of Physics of the Earth, Moscow, Russia. E-mail: vinnik@ijz.ru*

<sup>2</sup>*Department of Geological Sciences, University of Durham, Durham, DH1 3LE, UK*

<sup>3</sup>*Institute of Theoretical Geophysics, University of Cambridge, Cambridge, UK*

Accepted 2004 November 17. Received 2004 September 30; in original form 2004 April 21

## SUMMARY

To study the deep structure of Iceland, we conducted *S* receiver function analysis for almost 60 local broad-band seismograph stations of the Hotspot, ICEMELT and SIL networks. The structure was investigated separately for the central region of Iceland containing the neovolcanic zone and two peripheral regions to the east and west. *S*-to-*P* converted phases from upper-mantle discontinuities were detected by stacking recordings of several tens of teleseismic events. The analysis reveals previously unknown details. Magnitude and depth extent of the low *S* velocity anomaly in the upper mantle beneath Iceland are much larger than reported in earlier studies. Clear *S*-to-*P* converted phases are obtained from the discontinuity at a depth of  $80 \pm 5$  km, separating the high-velocity mantle lid from the underlying low *S* velocity layer. This discontinuity can be interpreted as a chemical boundary between dry harzburgite in the upper layer and wet peridotite underneath. Beneath peripheral parts of Iceland, we detect a boundary at a depth of  $135 \pm 5$  km with *S* velocity increasing downwards. This boundary may correspond to the onset of melting in wet peridotite at a potential temperature of around 1400 °C. Models of melting induced by CO<sub>2</sub> are not incompatible with our observations. The seismic data demonstrate effects that may be caused by azimuthal anisotropy in the upper mantle. There are indications of a second low *S* velocity layer to the NNE of Iceland, with the top near 480 km depth, similar to one recently detected beneath the Afro-Arabian hotspot.

**Key words:** hotspot, Iceland, mantle, receiver functions.

## 1 INTRODUCTION

Iceland is the type example of a ridge-centred hotspot and the mantle beneath has been studied in many seismic experiments. Global tomography (Ritsema *et al.* 1999) reveals a low *S* velocity anomaly in the mantle beneath Iceland that extends down into the transition zone, but the resolution of global tomography is low and the anomalies are strongly smoothed. Local teleseismic tomography (see Foulger *et al.* 2001 for a review) with a lateral resolution of 50–100 km reveals a low-velocity body beneath central Iceland in the depth range 100–400 km. Peak *P* and *S* velocities in this body are lower than beneath the periphery of Iceland by up to 3 and 5 per cent, respectively. Accordingly, Iceland can be divided into three major regions (Fig. 1): the central part, corresponding to the deep low-velocity body, and two peripheral regions to the east and west.

Recent analysis of *P* receiver functions (Du *et al.* 2004) demonstrates that all parts of Iceland are underlain by a low-velocity mantle layer, where the *S* velocity is reduced by up to approximately 10 per cent relative to standard Earth models such as IASP91 (Kennett

& Engdahl 1991). The low-velocity body beneath the central region is ~200 km across and extends into the transition zone. The 410-km discontinuity beneath this body is depressed by ~15 km. No topography is found on the 660-km discontinuity.

In the present paper, we describe new seismic constraints on the structure of the upper mantle beneath Iceland. To date, the only mantle discontinuities reported in this region are those bounding the transition zone at depths of ~410 and 660 km (e.g. Shen *et al.* 2002; Du *et al.* 2004). The lack of knowledge of other possible boundaries is a result of limitations of the *P* receiver-function technique: *P*s (*P*-to-*S*) converted phases from the uppermost mantle arrive in a time interval dominated by crustal reverberations. To avoid this obstacle, we use an alternative, *S* receiver-function technique, which is based on *Sp* (*S*-to-*P*) converted phases (Farra & Vinnik 2000). *Sp* converted phases from the upper mantle arrive earlier than crustal reverberations, which is a major advantage of the *S* receiver-function technique. This advantage has already been used in several studies (Oreshin *et al.* 2002; Vinnik & Farra 2002; Vinnik *et al.* 2004).

Our new seismic results have bearing on the problem of temperature and composition in the mantle beneath Iceland. The question of



**Table 1.** Estimates of potential temperature and temperature anomalies in the Iceland region.

Method	Potential temperature (°C) or temperature-anomaly (K) estimate	Depth (km)	References
<b>Seismology</b>			
Global and teleseismic tomography	Max 200 or 0 K and ~ 0.6 per cent partial melt (relative to MORs)	< ~200	(see Foulger <i>et al.</i> 2001, for a review)
Global and teleseismic tomography	~60 or 0 K and ~ 0.15 per cent partial melt (relative to MORs)	200–400	(see Foulger <i>et al.</i> 2001, for a review)
Depth of 660-km discontinuity	0 K (relative to average Earth–IASP91)	~660	(Du <i>et al.</i> 2004)
Depth of 410-km discontinuity	200 K or compositional anomaly of ~ 5 in Mg# and 100 K (relative to average Earth–IASP91)	~410	(Shen <i>et al.</i> 2002; Du <i>et al.</i> 2004)
<i>This study</i>	~50 K (relative to 1350 °C adiabat)	80–130	
<b>Petrology</b>			
Olivine–glass thermometry	1270 °C	~50	(Breddam 2002)
CMA5NF geothermometer & high-MgO glasses	1240–1260 °C (~0 K relative to MORs)	>60	(Gudfinnsson <i>et al.</i> 2003)
Major element systematics of Icelandic MORB	0 K (relative to MORs)	~50	(Presnall & Gudfinnsson 2004)
Picrite cumulates	1300 °C (~100 K relative to MORs)	~50	(Foulger <i>et al.</i> 2004)
<b>Other</b>			
Bathymetry of the North Atlantic	~70 K (relative to background)	< ~200	(Ribe <i>et al.</i> 1995)
Subsidence of ocean crust	50–100 K (relative to background)	<~200	(Clift 1997)
Uplift of Hebrides shelf	100 K (relative to background)	< ~200	(Clift <i>et al.</i> 1998)
Heat flow	<200 K (relative to background)	< ~200	(Stein & Stein 2003)
<b>Indirect estimates</b>			
Topography & length of geochemical anomaly	263 K		(Schilling, 1991)
Rare earth element inversions	100 K (relative to the Reykjanes ridge)		(White <i>et al.</i> 1995)

### 3 DATA

We processed seismograms recorded by 58 seismograph stations belonging to three broad-band networks deployed in Iceland, the SIL network and those of the Iceland Hotspot Project and ICEMELT (Stefánsson *et al.* 1993; Darbyshire *et al.* 1998; Foulger *et al.* 2001; Fig. 1). Microseismic noise with a period of 5–8 s is strong in Iceland and *S* waves are severely attenuated at periods of less than approximately 8 s. To attain a high signal-to-noise ratio, the raw recordings were low-pass filtered with a corner period of 8 s. Usable seismic events with magnitude not less than 6.0 in the epicentral distance range 60–100° form two groups each comprising nearly 30 events, one with a WSW backazimuth (average around 250°, events from

South America) and the other with a NNE backazimuth (average around 15°, events from east Eurasia). These two groups were processed separately and yielded somewhat different results.

Individual receiver functions were stacked to study the uppermost mantle beneath the eastern, western and central regions of Iceland separately. The surface projections of the piercing points of the *Sp* phases at depth *d* are shifted from the stations in the direction of the sources by a distance of approximately *d*. For each region, the projections of the wave paths of the *Sp* phases in the upper 100 km of the mantle lie mainly within the corresponding regions. Thus the stacks shown in Fig. 2 differ by region within Iceland and azimuth of approach of the waves. The numbers of seismograms stacked for each region and azimuth vary from 65 to 105. The reference

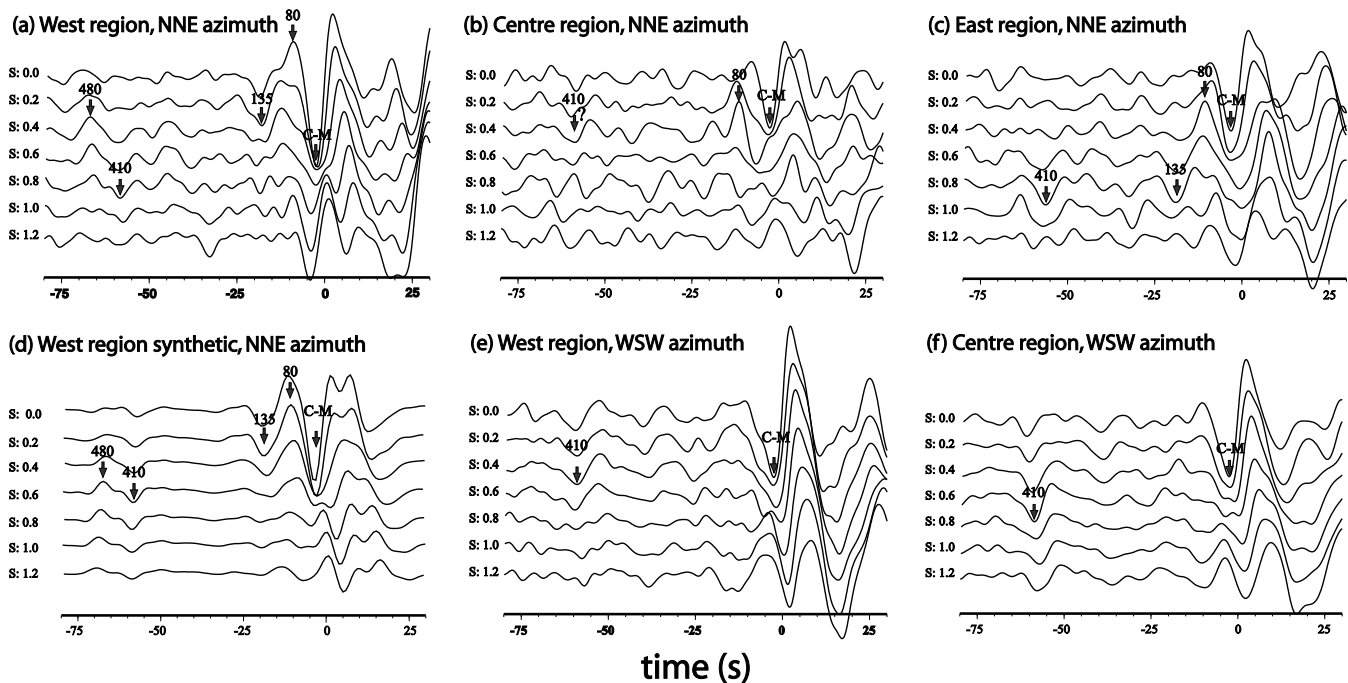


**Figure 2.** Stacked  $S$  receiver functions characterizing different regions and directions of wave propagation: (a) western region, NNE backazimuth, 100 recordings; (b) central region, NNE backazimuth, 65 recordings; (c) eastern region, NNE backazimuth, 78 recordings; (d) synthetic stack for the western region, NNE backazimuth; (e) western region, WSW backazimuth, 65 recordings; (f) central region, WSW backazimuth, 105 recordings. The  $S$  velocity model used to generate the synthetic stack in (d) is shown in Fig. 3 (Iceland). The numbers from 0.0 to 1.2 are differential slowness for the corresponding traces in  $\text{s deg}^{-1}$ . Arrows indicate seismic arrivals discussed in the text and the corresponding numbers indicate the depths deduced for the related discontinuities. The arrows point to the traces with the largest amplitudes. C–M denotes the crust–mantle boundary. Because the piercing points are displaced from the receivers in the directions of the epicentres of the seismic events, the  $S_p$  phases from the events from the WSW at the eastern stations mostly characterize the upper mantle not of the eastern but of the central region. For this reason, the stack for the eastern region is not shown.

distance varies between the stacks but is always close to  $78^\circ$ . The rms amplitudes of random noise, normalized to the amplitudes of the parent  $SV$ , vary from 0.006 (for the western region, NNE backazimuth and the central region, WSW back azimuth) to 0.009 (for the eastern and central regions, NNE back azimuth). The amplitudes of the signals detected are several times the rms amplitude of the noise.

All the stacks contain strong signals with negative polarity at approximately  $-3.5$  s. This is the  $S_p$  phase corresponding to the crust/mantle transition at a depth of  $\sim 30$  km (Foulger *et al.* 2003). Another prominent signal with a negative polarity arrives at approximately  $-59$  s and corresponds to the global discontinuity at a depth of  $\sim 410$  km. Other features of importance are seen only in the stacks corresponding to the NNE back azimuth (Figs 2a–c), which is the approximate strike of the mid-Atlantic ridge. For this backazimuth, a signal with positive polarity arrives at a time of around  $-12$  s (Figs 2a–c) in all regions. It is especially well pronounced in the central and eastern regions. The amplitude of this signal normalized to the amplitude of the parent  $SV$  is  $\sim 0.06$ , which is well above the noise. This is the  $S_p$  phase from the boundary between a high-velocity mantle lid and an underlying low-velocity layer at a depth of  $80 \pm 5$  km. Both the input signal and the converted phase from the crust/mantle boundary have a large central lobe and smaller side lobes, and the crustal side lobes could be mistaken for the main lobes of other signals. However, the signal at  $-12$  s cannot be explained as a side lobe of the crustal signal as it is too strong and arrives in the central and eastern regions at a slowness of  $0.4 \text{ s deg}^{-1}$ , very different from the slowness of the crustal converted phase ( $0.0 \text{ s deg}^{-1}$ ).

A prominent signal with negative polarity is detected in the peripheral regions at a time of approximately  $-19$  s, arriving with a differential slowness of  $0.2 \text{ s deg}^{-1}$  in the western region and  $0.6\text{--}0.8 \text{ s deg}^{-1}$  in the eastern region (Figs 2a and c). The related positive discontinuity (velocity increasing downwards) lies at a depth of  $135 \pm 5$  km. The differential slowness of the signal in the western region is close to the theoretical value for a horizontal boundary, but in the east it is larger by  $0.5 \text{ s deg}^{-1}$ . The larger value could be explained by the boundary dipping to the SSW at an angle of approximately  $5^\circ$ . The larger value could also be an effect of laterally varying velocity in a layer between the surface and the horizontal boundary, but this is unlikely because then a similar effect would be present in other detected signals, which is not the case. The stack for the western region also contains a prominent signal with positive polarity at a time of approximately  $-67.5$  s. This signal could be generated at a depth of  $480 \pm 5$  km from a boundary where the  $S$  velocity decreases downwards.

The observed wavefield was modelled using a method based on a reflectivity technique (Vinnik *et al.* 2004). The synthetic stack for the western region for the NNE backazimuth (Fig. 2d) reproduces the main features of the actual stack (Fig. 2a). The corresponding  $S$  velocity model (Fig. 3) contains a high-velocity lid and an underlying low  $S$  velocity layer. The model was found by assuming two low-velocity regions: one in the uppermost mantle and the other in the transition zone. The parameters of the model were adjusted to make them compatible with the traveltimes and amplitudes of the detected phases. The upper boundary of the upper low-velocity layer at a depth around  $80$  km and the boundary at around  $135$  km depth correspond to the  $S_p$  phases at  $-12$  and  $-19$  s. The  $S$  velocity

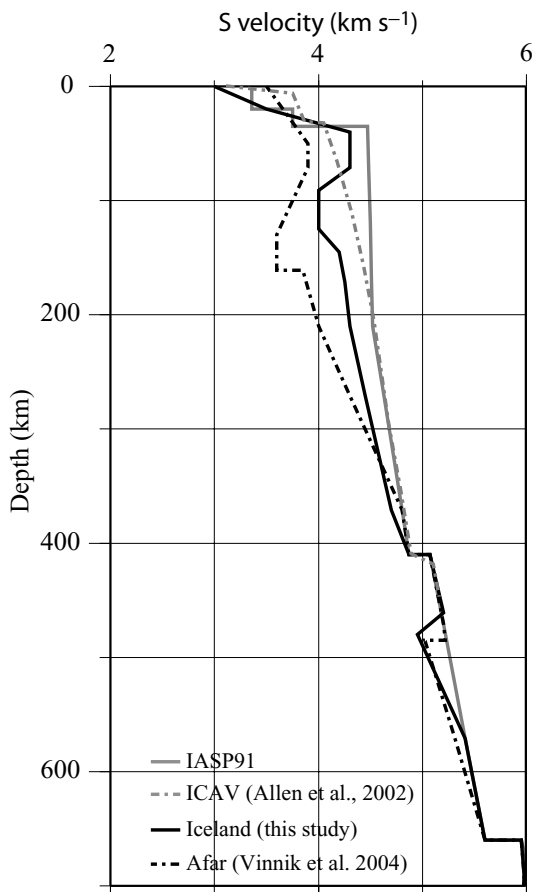


**Figure 3.**  $S$  velocity models: Iceland, the best-fitting model for the western region using synthetic modelling of the data from the NNE backazimuth (Figs 2a and d); Afar, the best-fitting model for the mantle beneath the Afro-Arabian hotspot (Vinnik *et al.* 2004); ICAV, the model derived from average phase velocity of surface Love waves across Iceland (Allen *et al.* 2002); IASP91, the IASP91 global model (Kennett & Engdahl 1991).

contrasts at these and the other boundaries are constrained by the signs and amplitudes of the respective converted phases. The  $S$  velocity anomaly of approximately  $-10$  per cent between 80 and 135 km depths is not sufficient to explain the time of the 410-km phase and in the model the low velocity extends practically to the 410-km discontinuity. The anomaly of approximately  $-10$  per cent is determined with an error of the order of  $\pm 1$  per cent. A low-velocity zone with its top at a depth around 480 km explains the signal at  $-67.5$  s. The data cannot distinguish between a sharp discontinuity with a thickness of a few kilometres and a gradational layer a few tens of kilometres thick. In the case of a gradational layer, the depth estimate we obtain corresponds to the middle of the layer.

#### 4 DISCUSSION

Our velocity model of the mantle beneath Iceland is very different from that by Allen *et al.* (2002) based mainly on the phase velocities of long-period surface waves (Fig. 3): the magnitude of the velocity reduction in our model is much larger and it extends to a larger depth. Insufficient resolution of the data used previously is the most likely reason for the discrepancy. A striking difference in the observed traveltime residuals of the  $Ps$  converted phases at Iceland and those predicted from Allen *et al.* (2002) is also reported by Du *et al.* (2004).

We detect a high-velocity lid beneath all parts of Iceland. The boundary between the lid and the underlying low-velocity layer is found everywhere at about the same depth, i.e. at  $\sim 80$  km. A similar boundary is present beneath the Pacific (Revenaugh & Jordan 1991; Gaherty *et al.* 1996), although at a shallower depth (60–70 km). A likely composition of the lid is peridotite depleted of water during MOR melting (Gaherty *et al.* 1996; Hirth & Kohlstedt 1996), whereas the low-velocity underneath the lid is most likely caused by the effect of water on anelastic relaxation (Karato 1995; Karato & Jung 1998). MOR melting may also result in partial elimination of basalt from the lid. If the lid is depleted in basalt, this basalt must reside in the overlying crust. This suggests that a relationship may exist between the thickness of the crust and the underlying lid. However, the thickness of the lid is about the same beneath both Iceland and the Pacific (around 50 km), but the crustal thickness differs greatly (up to 40 km in Iceland compared with 7 km in the Pacific). This implies different relationships between crustal thickness and mantle structure in Iceland and the Pacific.

The reduction of  $S$  velocity in the low-velocity layer by approximately 10 per cent relative to the IASP91 global model (Kennett & Engdahl 1991) cannot be explained by elevated temperature alone in a dry upper mantle, as an anomaly approaching  $600$  °C would then be required (Goes *et al.* 2000). It is possible in wet peridotite with a lowered solidus temperature, however. A large velocity reduction can be caused by temperature coming close to the solidus temperature. The discontinuity at 130–140 km depth may therefore correspond to the intersection of the mantle adiabat with the wet solidus. This explanation implies that the layer above the discontinuity contains melt. This discontinuity has not previously been observed in normal oceanic mantle, but it has been detected beneath the Afro-Arabian hotspot at a depth of 160 km (Vinnik *et al.* 2004). Apparently, a strong seismic signal can only be observed if the geotherm reaches the solidus.

Using the calibration curves proposed by Hirth & Kohlstedt (1996; their fig. 3) the temperature at a depth of 160 km beneath the Afro-Arabian hotspot was estimated by Vinnik *et al.* (2004) to be  $\sim 1550$  °C, or  $120$  °C higher than the temperature adopted by Hirth & Kohlstedt (1996) for MORs at this depth. Applying the same reasoning gives beneath peripheral regions of Iceland a potential temperature of  $\sim 1400$  °C, or  $\sim 50$  °C higher than that assumed by Hirth and Kohlstedt for MORs. A higher mantle temperature beneath the Afro-Arabian hotspot is consistent with the lower  $S$  velocity there (Fig. 3). Variations in water content could also affect the depth of onset of wet melting. The water content in the upper mantle beneath Iceland is poorly known, however, and the most recent estimate is  $\sim 600$ – $900$  ppm (Nichols *et al.* 2002). Variation in water content within this range could account for up to  $\sim 15$  km variation in the depth of onset of melting.

The effect of water on the solidus of peridotite may have been overestimated in earlier studies, and the low-velocity zone beneath oceans has recently been attributed to lowering of the peridotite solidus by the presence of  $\text{CO}_2$  (Presnall & Gudfinnsson 2004 and references therein). This model estimates the potential temperature in the upper mantle beneath Iceland to be  $\sim 1240$ – $1260$  °C. It does not predict the discontinuity we observe at a depth of 130–140 km and the upper boundary of the low-velocity layer is predicted to be at  $\sim 60$  km rather than the  $\sim 80$  km we observe. Nevertheless, given the uncertainties in the petrological model and the possibility of spatial variations in  $\text{CO}_2$  content, the theory of Presnall & Gudfinnsson (2004) is not necessarily incompatible with our observations.

So far, indications of a low-velocity layer with its top at approximately 480 km depth have been found only in the regions of Iceland

and the Afro-Arabian hotspot. Vinnik *et al.* (2004) suggested that beneath the Afro-Arabian hotspot this layer corresponds to the head of a plume trapped in the transition zone. A similar depth for these features in the two regions may be a coincidence or an indication of a common process. Further evidence for this feature could be sought by analysing *P* receiver functions, but in order to do so seismograph stations located approximately 500 km NNE of Iceland would be required.

The difference in the wavefields between the two backazimuths is indicative of azimuthal anisotropy, but current estimates of mantle anisotropy beneath Iceland with the fast direction around S–N (e.g. Li & Detrick 2003) are not very helpful in this respect. An explanation for the difference in terms of seismic anisotropy requires that the anisotropy is different in the 80–135 km layer and the upper mantle outside. For example, a model with a ridge-perpendicular fast direction in the layer and a ridge-parallel direction outside the layer might explain the observations. Future studies of mantle anisotropy with a higher resolution may show if such a model is consistent with the seismic data.

## ACKNOWLEDGMENTS

This research was supported by Natural Environment Research Council (NERC) grant GR3/10727 and a Sir James Knott Foundation fellowship held by GRF. LPV was supported by Russian Fund for Basic Research (RFBR) grant 04-05-64634. Parts of the digital seismic data were provided by the Incorporated Research Institutions for Seismology (IRIS) Data Management Center and the Icelandic Meteorological Office. The authors appreciate the comments from two anonymous reviewers.

## REFERENCES

- Allen, R.M. *et al.*, 2002. Imaging the mantle beneath Iceland using integrated seismological techniques, *J. geophys. Res.*, **107**(B12), 2325, doi:10.1029/2001JB000595.
- Anderson, D.L., 2000. The thermal state of the upper mantle; No role for mantle plumes, *Geophys. Res. Lett.*, **27**, 3623–3626.
- Breddam, K., 2002. Kistufell: Primitive melt from the Iceland mantle plume, *J. Petrol.*, **43**, 345–373.
- Clift, P.D., 1997. Temperature anomalies under the northeast Atlantic rifted volcanic margins, *Earth planet. Sci. Lett.*, **146**, 195–211.
- Clift, P.D., Carter, A. & Hurford, A.J., 1998. The erosional and uplift history of NE Atlantic passive margins: constraints on a passing plume, *J. geol. Soc. Lond.*, **155**, 787–800.
- Darbyshire, F.A., Bjarnason, I.T., White, R.S. & Flovenz, O.G., 1998. Crustal structure above the Iceland mantle plume imaged by the ICEMELT refraction profile, *Geophys. J. Int.*, **135**, 1131–1149.
- Du, Z., Vinnik, L.P. & Foulger, G.R., 2004. Evidence from *P*-to-*S* mantle converted waves for a flat ‘660-km’ discontinuity beneath Iceland, *Earth planet. Sci. Lett.*, submitted.
- Farra, V. & Vinnik, L., 2000. Upper mantle stratification by *P* and *S* receiver functions, *Geophys. J. Int.*, **141**, 699–712.
- Foulger, G.R. & Natland, J.H., 2003. Is ‘hotspot’ volcanism a consequence of plate tectonics?, *Science*, **300**, 921–922.
- Foulger, G.R. *et al.*, 2001. Seismic tomography shows that upwelling beneath Iceland is confined to the upper mantle, *Geophys. J. Int.*, **146**, 504–530.
- Foulger, G.R., Du, Z. & Julian, B.R., 2003. Icelandic-type crust, *Geophys. J. Int.*, **155**, 567–590.
- Foulger, G.R., Natland, J.H. & Anderson, D.L., 2004. Genesis of the Iceland Melt Anomaly by Plate Tectonic Processes, in Foulger, G.R., Natland, J.H., Presnall, D.C. & Anderson, D.L., eds, *Plates, Plumes & Paradigms*, Geological Society of America.
- Gaherty, J.B., Jordan, T.H. & Gee, L.S., 1996. Seismic structure of the upper mantle in a central Pacific corridor, *J. geophys. Res.*, **101**, 22 291–22 309.
- Goes, S., Govers, R. & Vacher, P., 2000. Shallow mantle temperatures under Europe from *P* and *S* wave tomography, *J. geophys. Res.*, **105**, 11 153–11 169.
- Gudfinnsson, G., Presnall, D.C. & Oskarsson, N., 2003. Contrasting origins of the most magnesian glasses from Iceland and Hawaii. In: Foulger, G.R., Natland, J.H. & Anderson, D.L., eds, *Plume IV: Beyond the Plume Hypothesis*, Hveragerdi, Iceland, August 2003, Hveragerdi, Iceland. Geological Society of America.
- Hirth, G. & Kohlstedt, D.L., 1996. Water in the oceanic upper mantle: Implications for rheology, melt extraction and the evolution of the lithosphere, *Earth planet. Sci. Lett.*, **144**, 93–108.
- Karato, S.-I., 1995. Effect of water on seismic velocities in the upper mantle, *Proc. Japan. Acad. Sci.*, **B 71**, 61–66.
- Karato, S. & Jung, H., 1998. Water, partial melting and the origin of the seismic low velocity and high attenuation zone in the upper mantle, *Earth planet. Sci. Lett.*, **157**, 193–207.
- Kennett, B.L.N. & Engdahl, E.R., 1991. Travel times for global earthquake location and phase identification, *Geophys. J. Int.*, **105**, 429–466.
- Li, A.B. & Detrick, R.S., 2003. Azimuthal anisotropy and phase velocity beneath Iceland: implication for plume-ridge interaction, *Earth planet. Sci. Lett.*, **214**, 153–165.
- McKenzie, D. & Bickle, J., 1988. The volume and composition of melt generated by extension of the lithosphere, *J. Petrol.*, **29**, 625–679.
- Nichols, A.R.L., Carroll, M.R. & Hoskuldsson, A., 2002. Is the Iceland hot spot also wet? Evidence from the water contents of undegassed submarine and subglacial pillow basalts, *Earth planet. Sci. Lett.*, **202**, 77–87.
- Oreshin, S., Vinnik, L., Peregoudov, D. & Roecker, S., 2002. Lithosphere and asthenosphere of the Tien Shan imaged by *S* receiver functions, *Geophys. Res. Lett.*, **29**, doi:10.1029/2001GL014441.
- Presnall, D.C., 1995. Phase diagrams of Earth-forming minerals, in *Mineral Physics and Crystallography: A Handbook of Physical Constants*, pp. 248–268, Ahrens, T.J., ed., American Geophysical Union, Washington, DC.
- Presnall, D.C. & Gudfinnsson, G.H., 2004. Potential temperatures at ridges and associated ‘hot spots’: Low velocity zone constraints, in Foulger, G.R., Natland, J.H., Presnall, D.C. & Anderson, D.L., eds, *Plates, Plumes & Paradigms*, Geological Society of America.
- Revenaugh, J. & Jordan, T.H., 1991. Mantle layering from ScS reverberation 3. The upper mantle, *J. geophys. Res.*, **96**, 19 781–19 810.
- Ribe, N.M., Christensen, U.R. & Theissing, J., 1995. The dynamics of plume-ridge interaction, 1: Ridge-centered plumes, *Earth planet. Sci. Lett.*, **134**, 155–168.
- Ritsema, J., van Heijst, H.J. & Woodhouse, J.H., 1999. Complex shear wave velocity structure imaged beneath Africa and Iceland, *Science*, **286**, 1925–1928.
- Schilling, J.-G., 1991. Fluxes and excess temperatures of mantle plumes inferred from their interaction with migrating mid-ocean ridges, *Nature*, **352**, 397–403.
- Shen, Y. *et al.*, 2002. Seismic evidence for a tilted mantle plume and north-south mantle flow beneath Iceland, *Earth planet. Sci. Lett.*, **197**, 261–272.
- Stefánsson, R. *et al.*, 1993. Earthquake prediction research in the south Iceland seismic zone and the SIL project, *Bull. seism. Soc. Am.*, **83**, 696–716.
- Stein, C. & Stein, S., 2003. Sea floor heat flow near Iceland and implications for a mantle plume, *Astron. Geophys.*, **44**, 1.8–1.10.
- Vinnik, L. & Farra, V., 2002. Subcratonic low-velocity layer and flood basalts, *Geophys. Res. Lett.*, **29**(4), 1049, doi:10.1029/2001GL014064.
- Vinnik, L.P., Farra, V. & Kind, R., 2004. Deep structure of the Afro-Arabian hotspot from *S* receiver functions, *Geophys. Res. Lett.*, **31**(11), L11608, doi:10.1029/2004GL019574.
- White, R.S., Bown, J.W. & Smallwood, J.R., 1995. The temperature of the Iceland plume and origin of outward propagating V-shaped ridges, *J. geol. Soc. Lond.*, **152**(6), 1039–1045.